

Influence of the Gas-Water Interface on Transport of Microorganisms through Unsaturated Porous Media

JIAMIN WAN,^{1*} JOHN L. WILSON,¹ AND THOMAS L. KIEFT²

Department of Geoscience¹ and Department of Biology,² New Mexico Institute of Mining and Technology, Socorro, New Mexico 87801

Received 7 April 1993/Accepted 23 August 1993

In this article, a new mechanism influencing the transport of microorganisms through unsaturated porous media is examined, and a new method for directly visualizing bacterial behavior within a porous medium under controlled chemical and flow conditions is introduced. Resting cells of hydrophilic and relatively hydrophobic bacterial strains isolated from groundwater were used as model microorganisms. The degree of hydrophobicity was determined by contact-angle measurements. Glass micromodels allowed the direct observation of bacterial behavior on a pore scale, and three types of sand columns with different gas saturations provided quantitative measurements of the observed phenomena on a porous medium scale. The reproducibility of each breakthrough curve was established in three to five repeated experiments. The data collected from the column experiments can be explained by phenomena directly observed in the micromodel experiments. The retention rate of bacteria is proportional to the gas saturation in porous media because of the preferential sorption of bacteria onto the gas-water interface over the solid-water interface. The degree of sorption is controlled mainly by cell surface hydrophobicity under the simulated groundwater conditions because of hydrophobic forces between the organisms and the interfaces. The sorption onto the gas-water interface is essentially irreversible because of capillary forces. This preferential and irreversible sorption at the gas-water interface strongly influences the movement and spatial distribution of microorganisms.

Research on the fate and transport of microorganisms in the subsurface environment has been stimulated by interest in *in situ* biodegradation of contaminated soils and groundwater (23, 36), colloid-facilitated transport of radionuclides (6), and the enhancement of crude-oil recovery (7), etc. A traditional and important concern is also the disposal of sewage by infiltration through soil to remove pathogenic microorganisms. In studies of microorganisms as pollutants, researchers (17, 18) have pointed out that microorganisms travel from a contamination source through unsaturated soil to groundwater. In studies of microorganisms as bioremediation agents (8, 44), introduced microbes are required to be transported to and throughout the contaminated site, perhaps including transport through the unsaturated zone. All of these cases demand the ability to accurately predict the rate and extent of microbial transport through porous media. Predictive mathematical models need to build on a better understanding of the behavior of microorganisms in soils and groundwater.

Transport of microorganisms is governed by sorption to immobile substrates and also by inactivation (2, 14, 46). Many factors contributing to sorption have been studied: the nature of the porous medium, including soil type, grain size, heterogeneity, and clay and organic matter content (1, 3, 15, 28, 33); water chemistry, including pH and ionic strength (2, 24); cell types, including size and surface hydrophobicity (13, 15, 19, 38); infiltration rate (40); and clogging efficiency (37). Most transport studies have focused on saturated porous media, but a few have focused on unsaturated conditions. Lance and Gerba (22) found that unsaturated flow resulted in a lower degree of virus mass recovery through loamy sand. Powelson et al. (32, 33) reported that viruses were more strongly removed from the soil water under unsaturated than saturated condi-

tions, and they suggested that the unrecovered viruses were inactivated. Yates et al. (45) found temperature to be the only measured water characteristic significantly correlated with viral inactivation. All of the approaches currently used for modeling bacterial transport involve the use of an advection-dispersion equation modified to include growth, death, and a number of other processes (10, 11, 24, 31). The models are difficult to test empirically because of the large number of parameters describing geological and bacterial variability, the exact determination of which is impractical (15).

In unsaturated subsurface environments, gas is one of three major phases, solid, water, and gas. There are basically two interfaces, the gas-water and the solid-water interfaces. The interactions of microorganisms with the solid-water interface have been studied for decades, but the gas-water interface has been ignored. The objectives of this project were to reveal the roles of the gas-water interface on microbial transport and to examine the causes of increased retention of microorganisms in unsaturated porous media.

The approach taken in this research combines visualization with quantification. Two major variables were examined, cell surface hydrophobicity and the gas saturation of the porous media. Two strains of bacteria with different surface hydrophobicities were used to examine the effect of cell surface hydrophobicity on sorption. Three types of columns with strictly controlled gas saturations were used to test the effect of the gas-water interface on microbial retention. Cell suspensions were injected at one end of the column, and cell breakthrough was measured at the other end. Fully water-saturated columns served as controls; unsaturated columns with a continuous gas phase (~46% gas saturation) represented the vadose zone condition. Columns with capillary-trapped residual gas bubbles (~15% gas saturation) were used to illustrate the differences between fully saturated and pseudosaturated conditions. We found from the literature that some of the laboratory soil columns and field sites which were referred to as water

* Corresponding author. Present address: Lawrence Berkeley Laboratory, MS 50E, 1 Cyclotron Rd., Berkeley, CA 94720.

saturated might actually contain capillary-trapped gas as a residual nonwetting fluid phase; the large discrepancy in some of the previously published results may be caused by the inadvertent presence of residual gas bubbles.

The phenomena responsible for the data collected in the columns were observed in etched glass micromodels, a new method for directly visualizing bacterial behavior within a porous medium. Water-saturated micromodels served as controls, while micromodels with capillary-trapped residual gas bubbles permitted direct observation of the interaction of bacteria with the gas-water interface.

In addition to the gas-water system, we present an example of a non-aqueous-phase liquid (NAPL)-water system to demonstrate more potential applications of the micromodel technique. The oil-water interface has been studied since 1924 (23, 26, 27), but our method allows studies under dynamic fluid conditions. We tested the behavior of a strain with intermediate hydrophobicity on the NAPL-water interface by culturing the cells in the micromodel and then displacing the cell suspension by a cell-free solution.

MATERIALS AND METHODS

Glass micromodels. Glass micromodels are transparent networks of pores and constrictions that simulate some of the complexities of natural porous media. Micromodels are created by etching mirror images of a pore network pattern onto two glass plates which are then fused together. A pore network is composed of pore bodies connected by pore throats. In a micromodel, these pores have a complex three-dimensional structure although the network is only two-dimensional. Etched glass micromodels provide an excellent method to study the mechanisms controlling the transport and capillary trapping of organic liquids and particles, including microorganisms, because the structure of the pore network and the wettability of the system can be closely controlled. Micromodels have been used increasingly to study enhanced oil-recovery processes in the past 30 years. Mattax and Kyte (25) made the first etched glass networks; the approach was then significantly improved by application of photoetching techniques (12). Micromodel methods have been reviewed by Peden and Husain (30), Wilson et al. (43), Buckley (5), and Conrad et al. (9). To adapt the micromodel technique to subsurface microbiological research, we modified the previous technique by reducing pore sizes, thinning the glass plate, etching multiple micromodels in one glass plate, and using different lighting systems. The procedure for generating the micromodels used in this research was described by Wan (41). Four micromodels with the same pore network pattern were generated in one glass plate (Fig. 1). Multiple micromodel plates allow us to repeat an experiment by simply shifting to the adjacent nearly identical network. Figure 2 shows three pore network patterns. Figure 2a shows a saturated hexagonal pore network with pore sizes of 20 to 250 μm ; Fig. 2b is a microphotograph of an unsaturated quadrilateral pore network showing air trapped as residual air bubbles (pore sizes, 40 to 200 μm). These two network patterns contain 1,250 pore bodies each. A wider pore size distribution with random pore network connections is closer to that of natural porous media. Figure 2c is an unsaturated heterogeneous network showing continuous gas and water phases (pore sizes range from 20 to 400 μm). These micromodels contain only about 0.1 ml of pore total volume. The glass encloses each of the pores at the top and bottom as well as along the sides, as shown in Fig. 2. The third dimension is best visualized in Fig. 2c, along the tops of the air-filled pore channels.

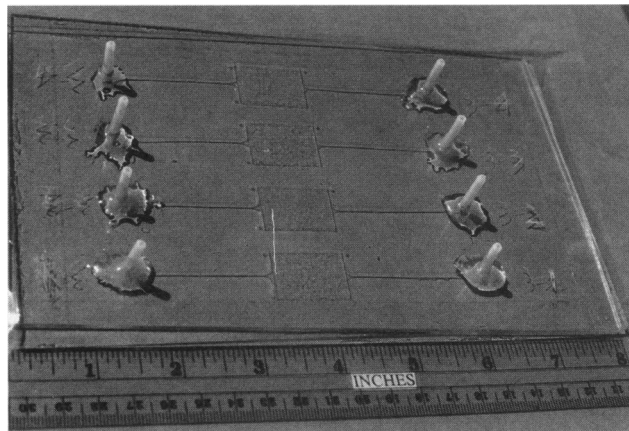


FIG. 1. Photograph of a glass multimicromodel plate containing four micromodels with a heterogeneous network pattern.

Solutions and cell suspensions. To simulate typical groundwater conditions (low ionic strength and approximately neutral pH), the ionic strength was 1.0 mM and the pH was 6.6 for all of the cell-free solutions and cell suspensions in all of the experiments. The electrostatic repulsive force was relatively large under these conditions; thus, minimal attachment of cells onto the solid-water interface was expected. The ionic strength of the solutions was adjusted with NaNO_3 , and the pH was buffered by NaHCO_3 . All chemicals used were analytical grade. Solutions were filtered through a 0.22- μm -pore-size filter before use. Cell suspensions were made in a filtered and autoclaved solution. Air was used as the gas phase, and isooctane was used as the NAPL.

Bacterial strains. Three bacterial strains were used in this research. *Arthrobacter* sp. (ZAL001, Subsurface Microbiology Culture Collection, Florida State University) was isolated by Kieft (21) from subsurface sediments (324-m depth). *Pseudomonas cepacia* 3N3A was isolated by Brockman et al. (4) from sediment samples at a depth of 203 m. These two strains were isolated from samples collected near the Savannah River Plant, near Aiken, S.C. *Arthrobacter* sp. strain S-139 was isolated by A. Mills et al. from a shallow groundwater aquifer. All three strains were used in micromodel experiments, but only 3N3A and S-139 were used in the column experiments. Cell size and cell surface characteristics are listed in Table 1. All of the measurements were carried out during the late stationary phase of growth. Cell size was measured with a phase-contrast optical microscope. Electrophoretic mobility was measured with a Coulter DELSA 440 (Doppler electrophoretic light scattering analyzer) in a solution of 1.0 mM NaNO_3 at pH 6.6. Mobility data were converted to zeta potentials (the surface potential within the double layer) calculated from the measured mean electrophoretic mobilities by using the tabulated numerical calculations of Ottewill and Shaw (29). A conventional method of estimating particle surface hydrophobicity is to use electrophoretic mobility or zeta potential, which is a measurement of surface charge state. However, surface charge density is not the sole factor controlling surface hydrophobicity. Surface contact-angle measurement is a better way to characterize the bacterial surface hydrophobicity. We used a modification of the contact-angle method of van Oss and Gillman (39) by employing a filter-layer-captive drop technique (16). A high-concentration bacterial suspension was filtered through a 0.45- μm -pore-size micropore filter. The filter, with a 50- to 100- μm -thick layer of bacteria, was fixed on

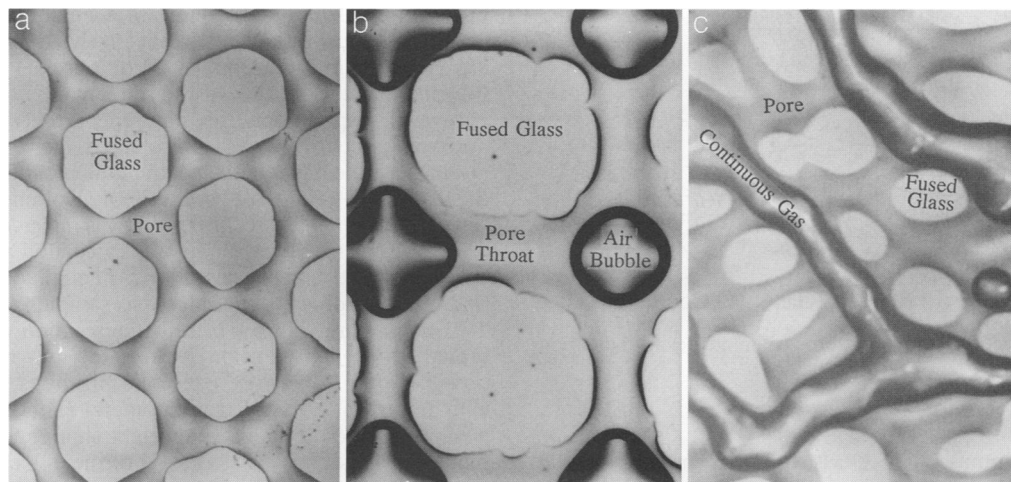


FIG. 2. Microphotographs of three types of networks showing different saturations, a saturated hexagonal network, pore size 20 to 250 μm (a), an unsaturated quadrilateral network with capillary trapped air bubbles, pore size 20 to 200 μm (b), and an unsaturated heterogeneous network with continuous gas phase, pore size 20 to 400 μm (c).

a glass slide. The slide was allowed to dry in a desiccator for 2 h. Contact angles were measured directly with a microscope (Carl Zeiss stereoscope) fitted with a goniometer eyepiece (no. 4443, Tiyoda, Tokyo, Japan) at the junction of the drop of the aqueous solution, the bacterial surface, and atmosphere at 24°C. The solution was 1.0 mM NaNO_3 (pH 6.6). The initial advancing contact angles are reported in Table 1. The readings were taken about 2 s after the water drop contacted the surface. Each reported contact angle is the mean of ≥ 15 measurements. There are several limitations in that the measured value depends on bacterial size, layer thickness, moisture content, and the recording time of the contact angle. This method is useful for measuring relative bacterial surface hydrophobicity under the same experimental conditions.

Bacteria were grown in a 10% PTYG broth at 27°C on a shaker. The broth contained the following ingredients per liter of distilled water (2a): 1.0 g of glucose, 1.0 g of yeast extract, 0.5 g of peptone, 0.5 g of tryptone, 0.6 g of $\text{MgSO}_4 \cdot 7\text{H}_2\text{O}$, and 0.07 g of $\text{CaCl}_2 \cdot 2\text{H}_2\text{O}$. When the culture reached a late logarithmic stage of growth (48 h), the cells were harvested by centrifugation ($5,000 \times g$, 10 min) and washed three times in a sterile solution of 1.0 mM NaNO_3 (pH 6.6). The cells were suspended in the same solution to a final concentration of about 5×10^{10} cells per ml and stored at 5°C. This concentrated cell suspension was used to make the cell film on the filter for the contact-angle measurement. In the micromodel and column experiments, the suspension was diluted to about 5×10^7 cells per ml in a solution of 1.0 mM NaNO_3 (pH 6.6).

Apparatus and procedure for the micromodel experiments. A high-resolution optical microscope with fluorescent lighting system, dark-field image, and long-working-distance objectives was used (Zeiss Axiophot). During the experiments, a pre-

pared micromodel was mounted horizontally on the stage of the microscope. The flow rate was controlled by a syringe pump (Harvard Apparatus model 4400-001). Photomicrographs and a video record were taken simultaneously.

Micromodel experiments involved the following procedural steps. (i) A new, clean micromodel was saturated by pumping distilled, deionized, and degassed water through it at as high a pumping rate as possible until all of the gas was removed or dissolved. (ii) A selected number of pore volumes of particle-free solution was pumped through the saturated micromodel to obtain the desired chemical conditions for the pore network. (iii) Air was trapped in the micromodel as residual bubbles by draining the micromodel with air and then displacing the air with aqueous solution. (iv) The micromodel was set on the microscope stage. A dilute cell suspension ($\sim 5 \times 10^7$ cells per ml) was injected at a constant rate (1.5 ml/h) for a preselected number of pore volumes (usually 30). The behavior of the bacteria was observed and recorded. (v) The cell suspension was replaced with a cell-free solution at the same flow rate until all of the free cells were displaced from the micromodel and only cells attached to solid-water and gas-water interfaces were left. (vi) The trapped gas bubbles were mobilized and subsequently removed from the network by increasing the pressure gradient (increasing the velocity of the water). (vii) In the NAPL-water experiments, isooctane (2,2,4-trimethylpentane) was used as the NAPL phase. Bacteria were cultured in a micromodel after step iii described above in a 1% PTYG broth for 48 h, and then step v followed (1% PTYG broth contained $0.1 \times$ concentration of organic components used in 10% PTYG broth but the same concentration of inorganic constituents).

Materials and procedure for the column experiments. Cy-

TABLE 1. Bacteria used in the experiments

Expt	Bacterial strain	Size (μm)	Contact angle (θ_a [°])	Zeta potential (mV)
Air-water micromodel and column	<i>P. cepacia</i> 3N3A	1.3×0.8	24.7 ± 3.1	-12.1
	<i>Arthrobacter</i> sp. strain S-139	1.0×0.8	77.1 ± 2.5	-56.3
Isooctane-water micromodel	<i>Arthrobacter</i> sp. strain ZAL001	1.1×0.8	48.2 ± 2.4	-46.2

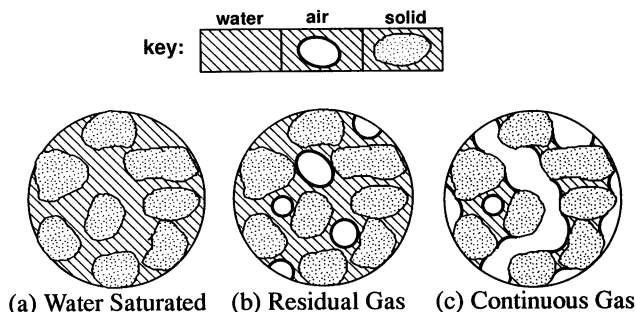


FIG. 3. Cross-sectional sketch of three column types with different saturations.

lindrical glass columns (ACE Glass, Inc.), 30 cm long and 2.5 cm in diameter, were used. The columns were packed with high-purity quartz sand (Unimin Co., New Canaan, Conn.) in grain sizes ranging from 212 to 315 μm in diameter. The purpose of choosing a narrow range of grain size was to gain relatively homogeneous packing and avoid layering. By using quartz sand instead of glass beads, we had better control of the chemical conditions of the solution. A clean medium surface is one of the most important factors in controlling the reproducibility of cell breakthrough data. The following cleaning procedure was used. Sand was soaked in 50% HNO_3 for 24 h and then washed with distilled water until the pH reached that of the distilled water. The sand was then soaked in a 1.0% (wt/vol) sodium polyphosphate solution and sonicated for 20 min. Polyphosphate can sequester calcium ion in a soluble or suspended form, thus detaching fine clay particles from sand surfaces. The sand was washed again with distilled water until the pH reached that of distilled water. The sand was sonicated in the solution of 1.0 mM NaNO_3 (pH 6.6) for 20 min and then washed with distilled deionized water five times. The sand was then dried in a clean oven at 110°C for 24 h. Columns were wet packed. Any remaining air trapped during packing was dissolved by flooding a degassed solution through the columns until complete water saturation was obtained (determined gravimetrically). Residual gas bubbles in the columns were created by draining the saturated columns and imbibing them with solution. The continuous gas phase was formed by draining the saturated column and then pumping a solution from the top of the column at a controlled rate, which resulted in an apparent seepage velocity of 10 cm/h. Figure 3 is a schematic illustration of the cross sections of three differently saturated columns. In Fig. 3a, the column is fully water saturated, and the quartz-water interface is the only interface present. In Fig. 3b, the column has about 15% gas saturation, with gas trapped as isolated bubbles. Two interfaces, the gas-water and solid-water interfaces, are present. In Fig. 3c, the column has about 46% gas saturation; both gas and water are interconnected and two interfaces exist. There were three to five repeated experiments for each combination of saturation and the two bacterial strains, for a total of almost 30 columns. The parameters for the column experiments were as follows: size of sand grains, 212 to 315 μm ; bulk density, $1.56 \pm 0.021 \text{ g/cm}^3$; porosity, 0.41 ± 0.005 ; residual gas saturation, $15.5 \pm 1.1\%$; continuous gas saturation, $46.5 \pm 2.0\%$; seepage velocity, 10.0 cm/h; ionic strength, 1.0 mM; pH, 6.65 ± 0.11 ; column weight changes, $-0.06 \pm 0.053\%$. These exact physical and chemical conditions ensured good reproducibility of breakthrough data. Each prepared column had precisely measured porosity (n), gas saturation (S_g), and water saturation (S_w). S_g and S_w represent

proportions of the void volume of a medium ($S_g + S_w = 1$) occupied by gas and water, respectively. A prepared column also had equilibrium chemical conditions (pH and turbidity of the effluent reached that of the influent).

In each experiment, the pumping rate Q (milliliters per hour) was set to match a preselected seepage velocity, $v = Q/AnS_w = 10 \text{ cm/h}$, where A is the bulk cross-sectional area of the column. A slug of 1 water pore volume of dilute cell suspension ($\sim 5 \times 10^7$ cells per ml) was injected at the seepage velocity. A water pore volume was calculated as S_wV , where V was the total column pore volume. The effluent was collected by a fraction collector at a rate of six samples per pore volume. Two water pore volumes of cell-free solution were injected to replace the cell suspension at the same flow rate. As soon as possible after collection, cell concentrations were measured with a double-beam spectrophotometer (Perkin-Elmer 330) at a wavelength of 260 nm. The weight change of the column at the end of a run as well as the pH of the effluent was checked. Each of our column experiments ran for 9 h, and sample analyses required approximately 1 h. A test of conditions conducted before the experiment showed that the cell concentration of the suspensions remained constant over 24 h at a room temperature of 24°C. This ensured that time was not a factor altering cell concentration during the experiment.

RESULTS AND DISCUSSION

Cell surface hydrophobicity. It has previously been suggested that the overall tendency of microorganisms to exhibit hydrophobic surface properties is determined by a complex interplay of polar and apolar outer surface components (35). Surface moieties that promote or reduce hydrophobicity appear to coexist on the cell surface. It is thus their relative concentration, distribution, configuration, and juxtaposition which determine the tendency of the cell to exhibit hydrophobic surface properties (34). Cell surface hydrophobicity is one of the most important factors governing the transport of microorganisms. During the past decade, investigators have implicated cell surface hydrophobicity in a wide variety of adhesion phenomena but have not related it to adhesion on gas-water interfaces. Cell surface hydrophobicity is poorly defined. The absence of a commonly accepted technique for the characterization of cell surface hydrophobicity is a potential problem in current research. In this article, we use water-air contact angles of cell surfaces to characterize the relative hydrophobicity. Table 1 lists the advancing contact angles, Θ_a , and electrostatic mobility data. Each water contact-angle value was the mean of 15 to 24 measurements. Contact angles are roughly inversely proportional to electrostatic mobilities.

Micromodel experiments. In the gas-water system experiments, we used two bacterial strains, hydrophilic strain 3N3A ($\Theta_a = 25^\circ$) and the relatively hydrophobic strain S-139 ($\Theta_a = 77^\circ$). Their behaviors at the gas-water and glass-water interfaces were visualized and recorded on videotape and photomicrographs. Figures 4 and 5 are photomicrographs taken after slugs of 30 pore volumes of dilute cell suspensions were injected and then replaced by a cell-free solution. Both photomicrographs were taken under transparent light and a bright field. Bacteria are shown as dark gray spots on the dark air-bubble surface (Fig. 2b shows a clean gas bubble and glass surface under the same lighting conditions). The ionic strength was 1.0 mM NaNO_3 (pH 6.6), and the flow rate was 1.5 ml/h. In Fig. 4, hydrophilic bacteria are preferentially sorbed onto a trapped gas bubble relative to the nearby glass pore walls. Only a few cells are sorbed onto the glass surface, mostly where the bubble and the pore walls form narrow throats. It is clear that the

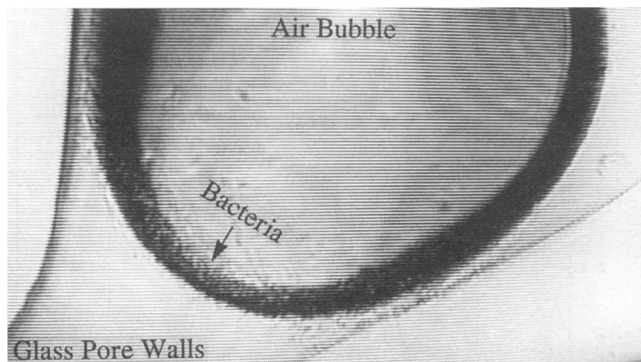


FIG. 4. Hydrophilic 3N3A bacteria (1.3 by 0.8 μm) preferentially sorbed on an air bubble trapped in a pore body of a hexagonal network. The air bubble is at the center and top, filling much of the frame. Bacteria are dark gray spots under the bright-field transparent light.

interfacial attractive energy between a gas bubble and a cell is greater than that between a glass wall and a cell. There is a greater tendency for bacteria to adhere to the gas-water interface than to the solid-water interface. In other words, the pair interaction energy of cell-air bubble is more attractive than that of cell-glass. For the cell-air bubble pair, both the electrostatic and van der Waals forces are repulsive. The only attractive force is the hydration force (20), and its absolute value must be greater than the sum of the repulsive forces. For the hydrophilic cell-glass pair, the electrostatic repulsive force is dominant and the total interaction energy is repulsive. The few cells sorbed on glass in the narrow throats may be due to their high velocity and collision rate. Cells with high-momentum energy may overcome the energy barrier and fall into the energy valley where van der Waals forces dominate. There may also be some straining in these narrow zones. In Fig. 5, relatively hydrophobic cells obviously have a greater affinity for the gas bubble as well as the glass surface than the hydrophilic cells in Fig. 4. The cell-bubble pair has more attractive energy because of the greater hydrophobic force between a cell and a gas bubble as the cell surface hydrophobicity increases. On the glass surface, the total interaction energy changes sign because of the increased hydrophobic force. In Fig. 5, the relatively hydrophobic cells have formed aggregates on both the gas-

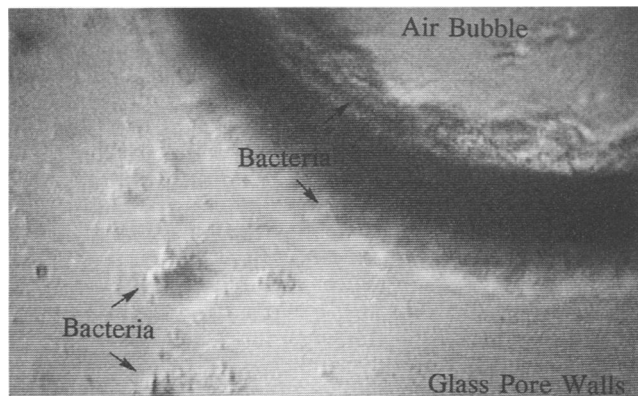


FIG. 5. Relatively hydrophobic S-139 bacteria (1.0 by 0.8 μm) accumulated on an air bubble and sorbed onto the pore wall in the pore body of a hexagonal network. The air bubble is on the upper right. The photograph was taken under a bright field and transparent light.

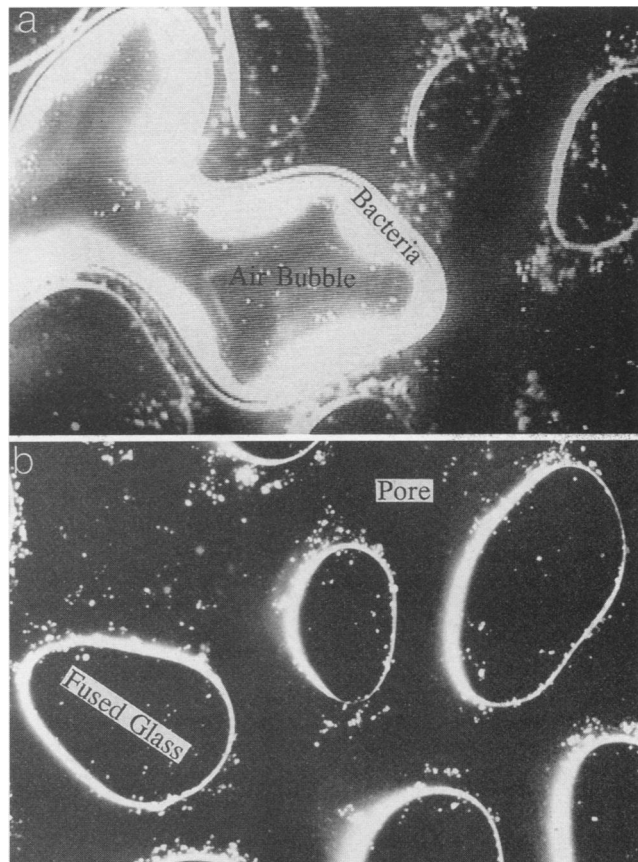


FIG. 6. Dark-field photographs with bacteria in white; heterogeneous network. (a) A large number of S-139 bacteria (1.0 by 0.8 μm) sorbed on a trapped air bubble and fewer bacteria sorbed on the pore walls. (b) The air bubble with sorbed bacteria removed by increasing water flow rate. Please note that, in Fig. 6 and 7, the dark field has highlighted blemishes (shown as big white spots) in the glass that may look like bacterial colonies. These can be seen in all sections of the model, including where the glass plates are completely fused, simulating a solid. The blemishes are visible only under a dark field.

water and glass-water interfaces. This formation is also due to the increased cell surface hydrophobicity.

In Fig. 6, relatively hydrophobic S-139 bacteria are shown in white on a dark field. Figure 2c shows this same heterogeneous pore network under transmitted light. In Fig. 6a, a large air bubble is trapped and almost covered by bacteria. This photo was taken after the cell suspension was flooded for 24 h (240 pore volumes) through the micromodel and then displaced by a cell-free solution. Some bacteria have sorbed on the pore walls, especially the side walls. This photograph convincingly demonstrates that bacteria prefer the gas-water interface to the glass-water interface. In Fig. 6b, the trapped air bubble with its sorbed bacteria has disappeared from the network and left behind a few cells sorbed onto the glass surface. This photograph was taken after step vi (described above); the residual air bubbles have been mobilized and carried away from the network by increasing the water flow rate. This experiment demonstrates that, for slow-flow conditions, the gas-water interfaces are static, behaving as collectors that inhibit the transport of bacteria. Shear stress induced by increased aqueous flow can mobilize the original static gas-water interface with the attached bacteria, thus enhancing

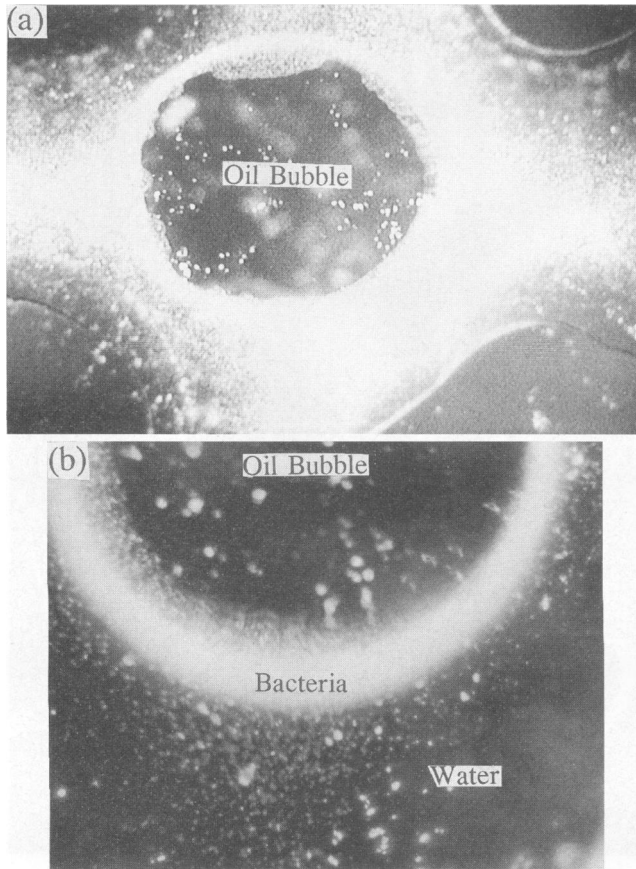


FIG. 7. Bacterial strain ZAL001 (1.1 by 0.8 μm) with a strong affinity to the organic carbon liquid-water interface (dark field). (a) Bacteria cultured in a quadrilateral network; (b) bacterial suspension displaced by bacteria-free solution after bacteria were cultured in a quadrilateral network. Bacteria remain on the oil-water interface. See legend to Fig. 6 for explanation of blemishes on the dark field.

bacterial transport. Natural events such as heavy rainfall or irrigation may enhance transport of particles, including bacteria, by mobilizing continuous gas-water interfaces.

Trapping isoctane in a quadrilateral network as the non-wetting phase and using bacterial strain ZAL001 ($\Theta_a = 48^\circ$), we have studied the behavior of microorganisms on the NAPL-water interface. In the dark-field photographs of Fig. 7, bacteria, in white, surround an oil drop trapped in a pore body. Figure 7a was taken after cells were cultured in a network in a solution of 1% PTYG for 48 h (we suggest a much lower concentration of PTYG in future experiments). This photo indicates that these bacteria prefer the aqueous phase to the oil phase. The bulk population of bacteria has not partitioned into the oil drop. Some of the bacteria have passed the three-phase contact line (glass, oil, and water) to enter the area of a thin water film at the top (toward the microscope) of the isoctane drop. This might result from the roughness of the glass surface where the water film between glass and isoctane is thick enough for the bacteria to enter. We also see a higher population of bacteria at the oil-water interface than in the bulk aqueous solution. This might result from the combination of the attractive pair energy of cell-oil bubble and the capillary force holding some cells on the oil-water interface. A capillary force holds the cells on the interface as long as the cells attach to the interface (42). In Fig. 7b, the cell suspension has been

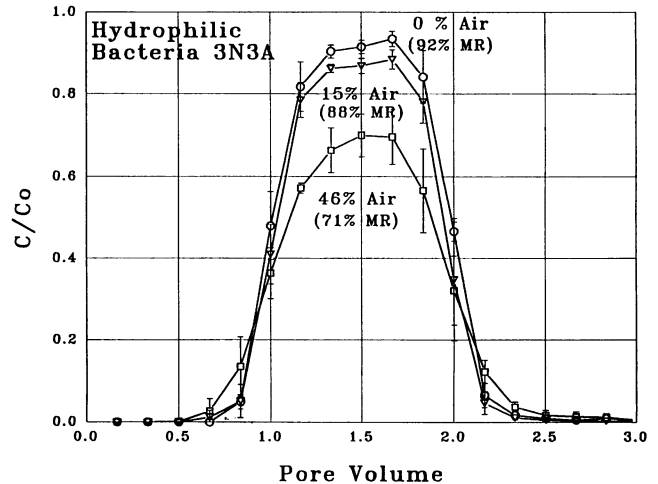


FIG. 8. Breakthrough curves of bacterial strain 3N3A from columns with three different saturations (three to five replications each). Percentages show the percentage of pore volume occupied by air (% Air) and the percentage of total cell mass recovery (% MR).

displaced by a cell-free solution. The cells on the oil-water interface remain; only the cells suspended in the aqueous solution have been removed. Some cells sorbed on the glass also remain behind. This photo indicates that, under these conditions, bacteria prefer the oil-water interface rather than the glass-water interface.

Column experiments. The same two strains used in the gas-water system micromodel experiments were used in the column experiments. A slug of 1 water pore volume of cell suspension was pumped from the top into the columns and then displaced by 2 water pore volumes of a particle-free solution at the same flow rate. Each strain was injected into the three types of columns with different saturations as described in Fig. 3. The results are presented as breakthrough curves where the fraction of the influent cell concentration leaving the packed column, C/C_0 , is a function of actual water pore volume. C and C_0 are the effluent and influent cell concentrations, respectively. The chemical conditions were the same as those in the micromodel experiments. For the three different saturation conditions, all the other experimental conditions were kept the same. Therefore, for a particular bacterial strain, the differences among the breakthrough curves are mainly caused by the presence and amount of gas.

Figures 8 and 9 summarize the data of the two respective strains, 3N3A and S-139. The solid lines represent the averages of the data from three to five repeated experiments. The standard deviation of each point is plotted as a vertical error bar. Figure 8 shows the breakthrough curves of hydrophilic 3N3A. The top curve is from the water-saturated columns, the middle curve is from the columns with a trapped residual gas phase, and the lower curve is from the columns with a continuous gas phase. The data show the following features. (i) The mass recoveries are inversely proportional to the gas saturations. Only 8% of the cells were lost in the fully-water-saturated columns, indicating unfavorable conditions for cell attachment to the solid surface, a fact which was consistent with the visualization demonstrated by the clean glass surface in Fig. 4. The 8% mass lost might have been caused by a mechanical filtration process, possibly by straining. Increasing the air saturation to the nonwetting phase residual (15.0%) lowered the mass recovery by 4%. Figure 4 suggests that the retained mass has been sorbed by the air bubbles trapped in the

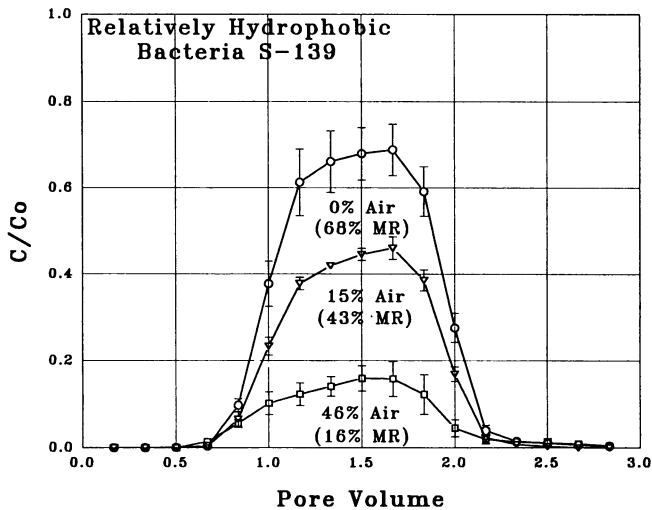


FIG. 9. Breakthrough curves of bacterial strain S-139 from columns with three different saturations (three to five replications each). Compare the effect of particle hydrophobicity on retention with the data in Fig. 8. For definitions of % Air and % MR, see the legend to Fig. 8.

pore bodies. Increasing the air saturation further to a continuous air phase decreased the mass recovery by 21% compared with that for water-saturated conditions. This difference was evidently caused by the increased area of the gas-water interface. These retained cells were sorbed onto the gas-water interface and in the narrow pore throats. (ii) The standard deviations in repeated experiments were small, relative to the difficulties usually encountered in reproducing data in filtration experiments. (iii) The seepage velocity was constant for the columns with different levels of water saturation. Columns were well packed (homogeneous), and no preferential advection was observed, even for the columns with a continuous gas phase. (iv) Slightly increased cell breakthrough dispersion with increased gas saturation is shown in Fig. 8. The moderate increase may have been due to a slight increase in water phase flow tortuosity induced by the presence of the gas. (v) The curves showed no tailing, indicating that sorption onto the gas-water interface is irreversible; in addition, any mechanically strained cells were not released. The irreversibility of sorption at the gas-water interface is presumably due to strong capillary forces (42).

Figure 9 shows the breakthrough curves of relatively hydrophobic bacteria from the three types of columns. All of the other experimental conditions were the same as those for the hydrophilic cells, and the cell sizes of the two strains were similar. The data indicate the following characteristics. (i) A higher proportion of hydrophobic cells than hydrophilic cells was retained in the columns. In the saturated conditions, 32% of the total cells were retained by sorption onto the solid surface of the medium as well as by mechanical straining. In the columns of trapped residual air, at least 25% of the cells sorbed onto the gas-water interface. In the columns with a continuous gas phase, at least 52% of the total mass was sorbed onto the gas-water interface. (ii) The lack of tailing indicates that sorption onto both interfaces as well as straining is irreversible. (iii) The relatively small error bars indicate the reproducibility of the data.

If we examine Fig. 8 and 4 together and Fig. 9 and 5 together, for each pair of figures we can observe the effect in one and the cause in the other. The data emphasize the importance of the gas-water interface on the transport of microorganisms in unsaturated porous media.

The glass micromodel technique allows us to determine the effect of the gas-water interface on the fate and transport of bacteria. This technique has the advantage of permitting direct observation of the behavior of bacteria on a pore and network scale under strictly controlled chemical and flow conditions. It has great potential to be used and further developed for additional purposes such as the optimization and monitoring of bioremediation processes and monitoring the functional activity of bacteria.

Although the column method has been commonly used in laboratory research, the effect of an inadvertent capillary-trapped gas phase has been neglected. We have demonstrated that certain conditions previously thought to be saturated may actually be pseudosaturated and contain gas trapped as a residual phase. For a relatively hydrophobic strain of bacteria, even a small amount of residual gas can dramatically reduce the transport. We have quantified bacterial sorption as a function of saturation conditions. In addition, the accurately controlled physical and chemical conditions of the column experiments have allowed us to achieve a greater degree of reproducibility than has been previously attained by other researchers by using the column methods.

The retention of microorganisms by porous media is in part a function of gas saturation due to preferential sorption onto the gas-water interface. Even relatively hydrophilic bacteria, which do not sorb onto the solid-water interface under unfavorable chemical conditions, are sorbed by the gas-water interface. The sorption appears to be due to the hydrophobic force: sorption at the gas-water interface increases with increasing particle hydrophobicity. It will be useful to test this hypothesis with other strains of relatively hydrophilic and hydrophobic bacteria. The sorption onto the gas-water interface also appears to be irreversible because of capillary forces. A static gas-water interface sorbs and retains microorganisms, thereby reducing their transport. A gas-water interface with previously sorbed cells can be mobilized and redistributed by the increased shear stress; the mobilized gas-water interface may thus increase the movement of microorganisms. The gas-water interface is a significant and previously unrecognized factor governing the movement and distribution of microorganisms in the subsurface environment, with potential applications that include in situ bioremediation, microbially enhanced oil recovery, and wastewater disposal.

ACKNOWLEDGMENTS

We acknowledge John McCarthy, Aaron Mills, and Jim Fredrickson for sharing their bacterial cultures and for their helpful discussion. We thank LuAnn Pavletich for help with editing the manuscript.

We also acknowledge the Subsurface Science Program, Office of Health and Environmental Research, U.S. Department of Energy, for supporting this work (DOE grant DE-FG03-92ER61484).

REFERENCES

- Bales, R. C., C. P. Gerba, G. H. Grondin, and S. L. Jensen. 1989. Bacteriophage transport in sandy soil and fractured tuff. *Appl. Environ. Microbiol.* **55**:2061-2067.
- Bales, R. C., S. R. Hinkle, T. W. Kroeger, and K. Stocking. 1991. Bacteriophage adsorption during transport through porous media: chemical perturbations and reversibility. *Environ. Sci. Technol.* **25**:2088-2095.
- Balkwill, D. L., and W. C. Ghiorse. 1985. Characterization of subsurface bacteria associated with two shallow aquifers in Oklahoma. *Appl. Environ. Microbiol.* **50**:580-588.
- Beven, K., and P. F. Germann. 1982. Macropores and water flow in soils. *Water Resour. Res.* **18**:1311-1325.
- Brockman, F. J., B. A. Denovan, R. J. Hicks, and J. K. Fredrickson. 1989. Isolation and characterization of quinoline-degrading

- bacteria from subsurface sediments. *Appl. Environ. Microbiol.* **55**:1029–1032.
5. Buckley, J. S. 1991. Multiphase displacements in micromodels, p. 157–189. In N. R. Morrow (ed.), *Interfacial phenomena in petroleum recovery*. Marcel Dekker, Inc., New York.
 6. Champ, D. R. 1986. Microbial mediation of radionuclide transport, p. 17. In F. H. Molz, J. W. Mercer, and J. T. Wilson (ed.), *Abstracts of the AGU Chapman Conference on Microbial Processes in the Transport, Fate, and In-Situ Treatment of Subsurface Contaminants*, Snowbird, Utah. American Geophysical Union, Washington, D.C.
 7. Chase, K. L., R. S. Bryant, K. M. Bertus, and A. K. Stepp. 1990. Investigations of mechanisms of microbial enhanced oil recovery by microbes and their metabolic products. U.S. Department of Energy report no. NIPER-483. U.S. Government Printing Office, Bartlesville, Okla.
 8. Claus, D., and N. Walder. 1964. The decomposition of toluene by soil bacteria. *J. Gen. Microbiol.* **36**:107–122.
 9. Conrad, S. H., J. L. Wilson, W. R. Mason, and W. J. Peplinski. 1992. Visualization of residual organic liquid trapped in aquifers. *Water Resour. Res.* **28**:467–478.
 10. Corapcioglu, M. Y., and A. Haridas. 1984. Transport and fate of microorganisms in porous media: a theoretical investigation. *J. Hydrol.* **72**:149–169.
 11. Corapcioglu, M. Y., and A. Haridas. 1985. Microbial transport in soils and groundwater: a numerical model. *Adv. Water Resour.* **8**:188–200.
 12. Davis, J. A., and S. C. Jones. 1968. Displacement mechanisms of micellar solutions. *J. Petrol. Technol.* **20**:1415–1428.
 13. Duncan-Hewitt, W. C. 1990. Nature of the hydrophobic effect, p. 39–74. In R. J. Doyle and M. Rosenberg (ed.), *Microbial cell surface hydrophobicity*. American Society for Microbiology, Washington, D.C.
 14. Fletcher, M. 1991. Bacterial colonization of solid surfaces in subsurface environments. In C. B. Fliermans and T. C. Hazen (ed.), *Proceedings of the First International Symposium on Microbiology of the Deep Surfaces*, p. 7-3–7-12. WSRC Information Services, Aiken, S.C.
 15. Fontes, D. E., A. L. Mills, G. M. Hornberger, and J. A. Herman. 1991. Physical and chemical factors influencing transport of microorganisms through porous media. *Appl. Environ. Microbiol.* **57**:2473–2481.
 16. Gaudin, A. M., A. F. Witt, and T. G. Decker. 1963. Contact angle hysteresis: principles and application of measurement methods. *Trans. AIME* **226**:107–112.
 17. Gerba, C. P. 1985. Microbial contamination of the subsurface, p. 53–67. In C. H. Ward, W. Giger, and P. L. McCarty (ed.), *Groundwater quality*. John Wiley & Sons, Inc., New York.
 18. Gerba, C. P., and S. M. Goyal. 1981. Quantitative assessment of the adsorptive behavior of viruses to soils. *Environ. Sci. Technol.* **15**:940–944.
 19. Grotenhuis, J. T. C., C. M. Plugge, A. J. M. Stams, and A. J. B. Zehnder. 1992. Hydrophobicities and electrophoretic mobilities of anaerobic bacterial isolates from methanogenic granular sludge. *Appl. Environ. Microbiol.* **58**:1054–1056.
 20. Israelachvili, J. N. 1992. *Intermolecular and surface forces*. Academic Press, Inc., New York.
 21. Kieft, T. L., and L. L. Rosacker. 1991. Application of respiration- and adenylate-based soil microbiological assays to deep subsurface terrestrial sediments. *Soil Biol. Biochem.* **23**:563–568.
 22. Lance, J. C., and C. P. Gerba. 1984. Virus movement in soil during saturated and unsaturated flow. *Appl. Environ. Microbiol.* **47**:335–337.
 23. Lee, M. D., J. M. Thomas, R. C. Borden, P. B. Bedient, J. T. Wilson, and C. H. Ward. 1988. Bioremediation of aquifers contaminated with organic compounds. *Crit. Rev. Environ. Control.* **18**:29–89.
 24. Martin, R. E., E. J. Bouwer, and L. M. Hanna. 1992. Application of clean-bed filtration theory to bacterial deposition in porous media. *Environ. Sci. Technol.* **26**:1053–1058.
 25. Mattax, C. C., and J. R. Kyte. 1961. Ever see a water flood? *Oil Gas J.* **59**:115–128.
 26. Mudd, S., and E. B. H. Mudd. 1924. The penetration of bacteria through capillary spaces. IV. A kinetic mechanism in interfaces. *J. Exp. Med.* **40**:633–645.
 27. Mudd, S., and E. B. H. Mudd. 1924. Certain interfacial tension relations and the behavior of bacteria in films. *J. Exp. Med.* **40**:647–660.
 28. Murphy, E. M., J. A. Schramke, J. K. Fredrickson, H. W. Bledsoe, A. J. Francis, D. S. Sklarew, and J. C. Linehan. 1992. The influence of microbial activity and sedimentary organic carbon on the isotope geochemistry of the Middendorf aquifer. *Water Resour. Res.* **28**:723–740.
 29. Ottewill, R. H., and J. N. Shaw. 1972. Electrophoretic studies of polystyrene lattices. *J. Electroanal. Interfacial Electrochem.* **37**:133–142.
 30. Peden, J. M., and M. Hussain. 1985. Visual studies in reservoir engineering: the development of a novel technique for the preparation of real pore space structure glass micromodels and their application in displacement experiments under simulated reservoir conditions, p. 37–48. Third European Meeting on Improved Oil Recovery, Rome, 16 to 18 April 1985.
 31. Peterson, T. C., and R. C. Ward. 1989. Development of a bacterial transport model for coarse soils. *Water Resour. Bull.* **25**:349–357.
 32. Powelson, D. K., J. R. Simpson, and P. Gerba. 1990. Virus transport and survival in saturated and unsaturated flow through soil columns. *J. Environ. Qual.* **19**:396–401.
 33. Powelson, D. K., J. R. Simpson, and P. Gerba. 1991. Effects of organic matter on virus transport in unsaturated flow. *Appl. Environ. Microbiol.* **57**:2192–2196.
 34. Rosenberg, M., and R. J. Doyle. 1990. Microbial cell surface hydrophobicity: history, measurement, and significance, p. 1–38. In R. J. Doyle and M. Rosenberg (ed.), *Microbial cell surface hydrophobicity*. American Society for Microbiology, Washington, D.C.
 35. Rosenberg, M., and E. Rosenberg. 1981. Role of adherence in growth of *Acinetobacter calcoaceticus* on hexadecane. *J. Bacteriol.* **148**:51–57.
 36. Thomas, J. M., and C. H. Ward. 1989. In situ bioremediation of organic contaminants in the subsurface. *Environ. Sci. Technol.* **23**:760–766.
 37. Vandevivere, P., and P. Baveye. 1992. Relationship between transport of bacteria and their clogging efficiency in sand columns. *Appl. Environ. Microbiol.* **58**:2523–2530.
 38. Van Loosdrecht, M. C. M., J. Lyklema, W. Norde, G. Schraa, and A. J. B. Zehnder. 1987. Electrophoretic mobility and hydrophobicity as a measure to predict the initial steps of bacterial adhesion. *Appl. Environ. Microbiol.* **53**:1898–1901.
 39. van Oss, C. J., and C. F. Gillman. 1972. Phagocytosis as a surface phenomenon. I. Contact angles and phagocytosis of non-opsonized bacteria. *J. Reticuloendothel. Soc.* **12**:283–292.
 40. Vaughn, J. M., E. F. Landry, C. L. Beckwith, and M. C. Thomas. 1981. Virus removal during groundwater recharge: effects of infiltration rate on adsorption of poliovirus to soil. *Appl. Environ. Microbiol.* **41**:139–147.
 41. Wan, J. 1993. The role of the gas-water interface on the transport of colloids and microorganisms in porous media. Ph.D. dissertation. New Mexico Institute of Mining and Technology, Socorro, N.M.
 42. Wan, J., and J. L. Wilson. Visualization of the role of the gas-water interface on the fate and transport of colloids in porous media. *Water Resour. Res.*, in press.
 43. Wilson, J. L., S. H. Conrad, W. R. Mason, W. Peplinski, and E. Hagan. 1990. Laboratory investigation of residual liquid organics from spills, leaks, and the disposal of hazardous waters in groundwater. EPA/600/690/004. R. S. Kerr Environmental Research Laboratory, U.S. Environmental Protection Agency, Washington, D.C.
 44. Wilson, J. T., L. E. Leach, M. Henson, and J. N. Jones. 1986. In situ bioremediation as a ground water remediation technique. *Ground Water Monit. Rev.* **6**:56–64.
 45. Yates, M. V., C. P. Gerba, and L. M. Kelly. 1985. Virus persistence in groundwater. *Appl. Environ. Microbiol.* **49**:778–781.
 46. Yates, M. V., S. R. Yates, J. Wagner, and C. P. Gerba. 1987. Modeling virus survival and transport in the subsurface. *J. Contam. Hydrol.* **1**:329–345.